



PII S0008-8846(97)00074-4

THE EFFECT OF MoO_3 ON THE C_3S AND C_3A FORMATION**V. Kasselouri and Ch. Ftikos**Department of Chemical Engineering of NTUA, Iroon Polytechniou 9,
Zografou Campus, Athens 15773, Greece

(Refereed)

(Received January 23, 1996; in final form April 3, 1997)

ABSTRACT

Using pure chemical reagents and varying the MoO_3 content (0-3.0w/w %) two series of eleven compositions, each for C_3S and C_3A phases, were prepared at 1450°C and investigated in respect of the molybdenum effect on the phases formed. Results derived by X-Ray Diffraction (XRD) and step by step XRD scanning technique reveal that MoO_3 addition, within the range examined, promotes both C_3S and C_3A formation. In both cases MoO_3 causes a remarkable increase of the crystal size. Higher than 1.0(w/w)% MoO_3 addition favours the formation of the monoclinic form of the C_3S phase. © 1997 Elsevier Science Ltd

Introduction

Many of the transition metal oxides are involved as minor constituents in the clinker raw meal and participate with an active way to transformation process, lowering consequently the energy demand. As a rule, their origin is derived from the accessory minerals of rocks, fuels, refractories, wear parts of equipment. They can also result from admixtures added to the raw meal for specific purposes.

The aims on stimulating the research regarding, generally, the minor constituents and admixtures for several years are:

- production of more reactive raw mixes
- improvement of particular technological conditions to increase the process efficiency
- increase in the allowable levels of impurities associated with enlargement of the availability of the raw materials and fuel types
- a way out to handle specific industrial wastes for ecological purposes
- improvement of the cement quality

The effect of the transition elements on the sintering of the clinker is attributed either to the temperature of the liquid phase formation and/or to the properties of the liquid phase, such as the viscosity, the surface tension and the diffusion coefficient. It is likely that these properties influence directly the reaction rate of the C_3S formation and the structure of the clinker phases as well (1-13).

Experimental data reported suggest that the effect of the transition element ions on the viscosity of the liquid phase mainly depends on their electronegativity and ionic radii. Thus,

ions having higher electronegativities and smaller ionic radii than the Ca^{2+} change the tetrahedral coordination of the Al^{3+} and Fe^{3+} to octahedral resulting in the decrease of viscosity. On the contrary, ions stabilising the tetrahedral coordination of the Al^{3+} and Fe^{3+} favour the replacement of the $(\text{SiO}_4)^{4-}$ tetrahedra by the $(\text{AlO}_4)^{5-}$ making then more stable networks Al-Si-O which cause an increase of viscosity. The addition of the transition elements in the liquid phase increases its viscosity according to following series $\text{Mo-W-Cr-Ti-Mn-Fe-Co-Cu-Ni-Zn-Cd}$ (11).

The diffusion coefficient of the solids, which affects the rate of the increase of the crystal size formed in the liquid phase, is directly determined by the temperature and its viscosity. Taking into account that the formation temperature of the liquid phase is not significantly varied, which is between 1280-1320°C for a majority of the clinkers, the diffusion coefficient mainly depends on the viscosity in a reversible function.

Furthermore, the presence of the d-elements affects the surface tension of the liquid phase. It is suggested that increase of the acidity of the d-elements results in a decrease of the surface tension proportional to the decrease of the viscosity already mentioned. The crystal form produced in the liquid phase, however, is determined by the surface tension at the solid-liquid interface depending on the adsorption of the foreign ions in the boundaries of the new crystal formed. Adsorption occurring at points with increased surfaced energy due to defects, holes or flaws causes a decrease of the surface tension and favours of smaller crystal production, while increased surface tension leads to larger and more spherical crystal formation. Particularly, at the final steps of the alite crystal development, the surface tension at the interface of the alite-liquid phase is more determined, than the diffusion coefficient, for the crystal rate development (12).

The sites that the ions of the d-elements occupy in the lattice of the clinker phases depend on their charge, ionic radius, polarity, coordination number, electronegativity and the structure of the host crystals. Generally, for the entrance of the d-ions in the clinker phases the following rules are suggested: ions having charge +2, large ionic radius and small polarity intend to replace Ca^{2+} . These having charge +4 and increased polarity normally replace the Si^{4+} . The replacements for ions having other charges is more complex, introducing a number of oxygen vacancies.

As far as the effects of the transition elements on the hydration properties of the cement produced are concerned they may lead to improvements, in the clinker activity due to the defects introduced in the crystal clinker phases, as the hydration kinetics of the clinker compounds is associated with an increase of the formation rate of the hydration products (14).

In an extended research programme we are attempting to investigate the effect of small additions of the transition metal oxides on the structure and properties of the main phases of the Portland cement clinker (8, 15). With the present paper we aim to elucidate the effect of MoO_3 on the formation and structure of the C_3S and C_3A phase, using X-Ray Diffraction (XRD) and step by step scanning XRD techniques. Our results show that the proper addition of MoO_3 promotes both the C_3S and the C_3A formation, increasing significantly their crystal size (D).

Experimental

Two series of compositions were prepared, each for C_3S and C_3A respectively, containing MoO_3 varied from 0.0 to 3.0%, by using pure chemical reagents. Pellets were formed from the well homogenised mixtures, calcined at 1000°C for 1 hour. Then the C_3S compositions

TABLE 1
The Series of the C₃S and C₃A Compositions Prepared

MoO ₃ content (%w/w)	Code of C ₃ S	Code of C ₃ A
0.0	S ₀	A ₀
0.1	S ₁	A ₁
0.2	S ₂	A ₂
0.3	S ₃	A ₃
0.4	S ₄	A ₄
0.5	S ₅	A ₅
0.75	S ₆	A ₆
1.0	S ₇	A ₇
1.5	S ₈	A ₈
2.0	S ₉	A ₉
3.0	S ₁₀	A ₁₀

were sintered at 1450°C for three hours, whilst the sintering conditions for the C₃A series were at 1450°C for 30 minutes. After sintering the samples were fast cooled in air. The code of the samples and the content of MoO₃ are referred to in the Table 1.

In order to identify the phases formed, the samples prepared were studied by means of XRD-analysis. XRD-analysis was performed by means of a Philips Diffractometer using CuK_α radiation. The diffractometer was operated at 40 kV and 25 mA. The XRD-spectra were obtained by scanning continuously at the rate of 1 °2θ/min.

Furthermore, the integrated intensities for the d-spacing of C₃S ($d = 2.614 \text{ \AA}$) and of C₃A ($d = 2.698 \text{ \AA}$) were calculated using step by step XRD scanning, operated in steps of 0.02° 2θ and measuring the counts per 20 seconds at each step. Integrated intensities obtained were used for the quantitative estimation and the crystal size (D) determination of both the C₃S and the C₃A phases. For the crystal size determination, the integral breadth of the diffraction peaks was used, applying then the Sherrer (16) equation ($D = k\lambda/\beta\cos\theta$, where λ : the wavelength in Å, β : the pure diffraction broadening, θ : the Bragg angle and k : constant, assuming to be 1.0 because the integral breadth is used).

Results and Discussion

Some representative XRD-patterns obtained for the S and A series are presented in Fig. 1. Results derived by XRD-analysis show qualitatively the formation of C₃S, β -C₂S phases, some γ -C₂S and CaO for the S series and C₃A, C₁₂A₇ phases, some CA and CaO for the A series. The peak intensities in the XRD-patterns support some qualitative comments for the phases formed. Thus, a remarkable increase of the C₃S phase is observed from the sample S₀ up to S₁₀. After the sample S₇ a transformation of the triclinic C₃S to monoclinic appears presented growing up to the sample S₁₀, revealing that MoO₃ additions up to 1(w/w) % promote C₃S in the triclinic form, whilst for higher concentrations, up to 3.0(w/w) % examined, favour the formation and stabilisation of the monoclinic form. In the case of the β -C₂S phase, it is not observed any significant difference of its peak intensities up to the samples S₆, appearing then an increase of this phase up to the sample S₁₀, which suggests that MoO₃ additions in the range of 1.0-3.0(w/w) % examined promote the β -C₂S phase formation. The

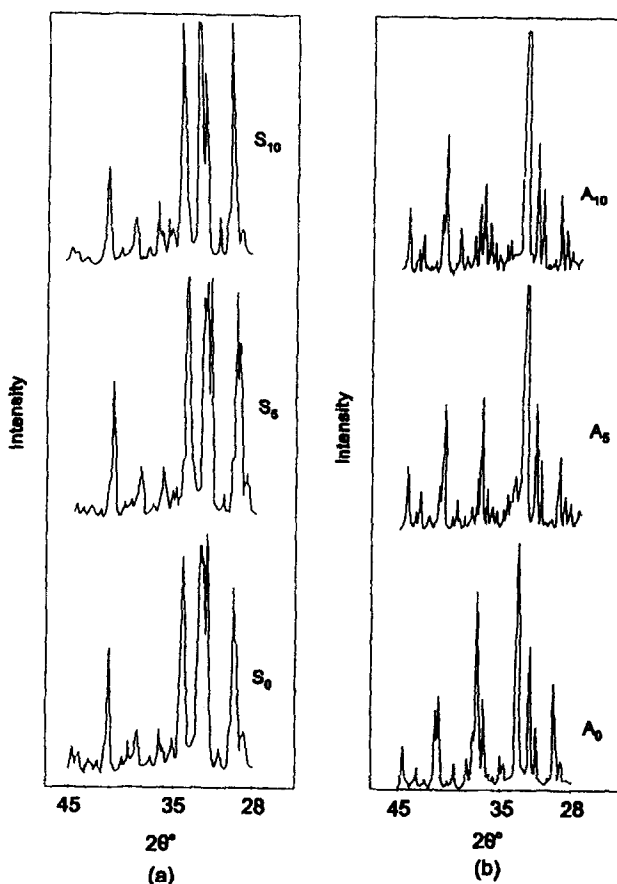


FIG. 1

Representative XRD-patterns of the samples prepared (a) S series, (b) A series.

same comments, as for the β - C_2S phase, one can note for the γ - C_2S phase, whose the presence may be mostly attributed to the non identical cooling conditions. As the MoO_3 additions increase a dramatic decrease of the CaO content is observed.

As for the A series, a remarkable increase of the C_3A phase is observed as the MoO_3 addition increases, up to 3.0(w/w) % examined, while no significant variations appear in the presence of the $C_{12}A_7$ and CA phases, the last being in a very low content. In this case, also, the CaO content decreases remarkably as the MoO_3 additions increase.

Figure 2 presents the integrated intensities calculated for C_3S (triclinic) ($d = 2.614 \text{ \AA}$) and C_3A ($d = 2.698 \text{ \AA}$) respectively, which does confirm the comments made above for these phases. The decrease of the C_3S phase after the sample S_7 is attributed to the partial transformation of the phase to the monoclinic form, weakening the diffraction peak intensity at $d = 2.614 \text{ \AA}$ and strengthening that of $d = 3.03 \text{ \AA}$.

Furthermore, the crystal size (D) for the C_3S (triclinic) and C_3A phases formed were calculated by applying the results derived from step by step XRD-analysis to the Scherrer

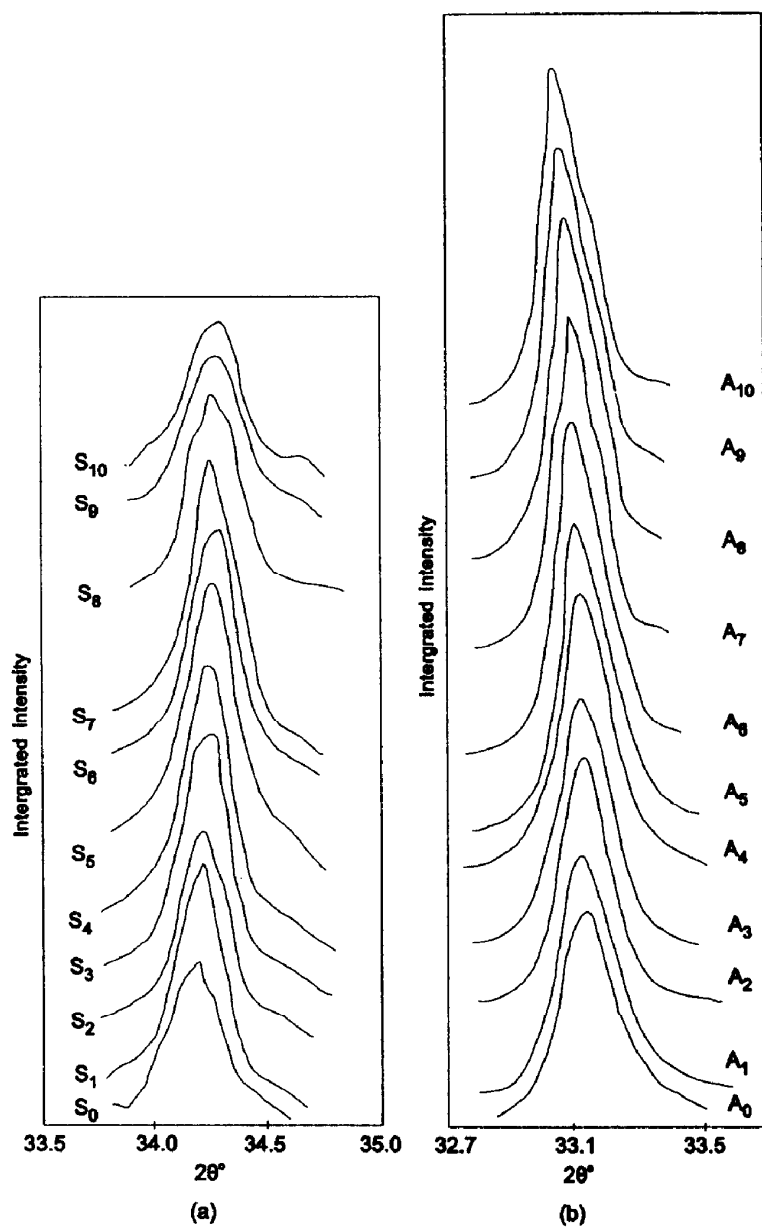


FIG. 2.
Integrated intensities for (a) C₃S ($d = 2.614 \text{ \AA}$), (b) C₃A ($d = 2.698 \text{ \AA}$).

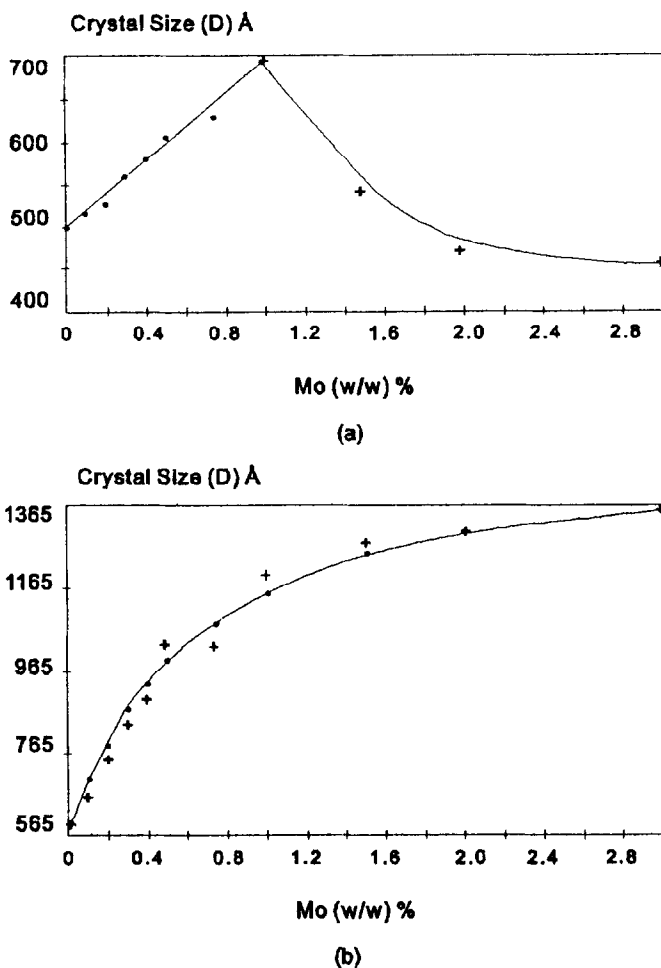


FIG. 3
Crystal size v. (w/w) % MoO_3 content for (a) C_3S , (b) C_3A .

equation (16, 17). Figure 3 shows plots of the crystal size (D) versus MoO_3 additions for the C_3S and C_3A respectively. The crystal size (D) in both the cases, is remarkably grown up to the percentage of 1.0(w/w) % MoO_3 content. The decrease of the C_3S crystal size observed, for the higher than 1.0(w/w) % MoO_3 additions, is attributed to the gradual change of the crystal form of the phase. In the case of the C_3A phase, addition of MoO_3 higher than 1.0(w/w) % increases gradually the crystal size of the phase, however, at a much slower rate.

Conclusions

The results derived by the present research work reveal that MoO_3 addition, within the range examined, promotes both the C_3S and the C_3A phase formation. In both cases the crystal size (D) increases remarkably up to 1(w/w) % MoO_3 content. For higher than 1(w/w) % MoO_3 addition, the crystal size of the C_3A increases gradually, however, at a slower rate, while in the C_3S case favours its transformation from the triclinic to monoclinic crystal form.

References

1. W.L. De Keyser, Proc. 8th Conf. of Silicate Ind., Budapest, 133 (1965).
2. H. Hornain, Rev. Mater. Constr., 203, 671-672 (1971).
3. I.A. Kryzanovskaya, Proc. 6th Int. Symp. on the Chemistry of Cement, Moscow, September (1974).
4. M. Enculescu, Proc. 6th Int. Symp. on the Chemistry of Cement, Moscow, September (1974).
5. M. Pezzuoli, Proc. 6th Int. Symp. on the Chemistry of Cement, Moscow, September (1974).
6. S.N. Ghosh, Proc. 6th Int. Symp. on the Chemistry of Cement, Vol. II, p.7-13, Paris (1980).
7. W.A. Klemm, Proc 7th Int. Symp. on the Chemistry of Cement, Vol. II p.1-150, Paris (1980).
8. V. Kasselouri, Ch. Ftikos and P. Psaris, Ciments Betons Plâtres Chaux, 781, 405 (1989).
9. M.S. Surana and S.N. Joshi, Zement Kalk Gips, 1 (1990).
10. R. Bucchi, Proc 7th Int. Symp. on the Chemistry of Cement, Vol. I pp.1-30, Paris (1980).
11. V.V Timachev and V.G. Akimov, Proc 7th Int. Symp. on the Chemistry of Cement, Vol. IV p.203, Paris (1980).
12. I. Maki, il Cemento, 4, (1984).
13. P. Fierens and J. Tirlocq, Cem. Concr. Research, 13 (1983).
14. G. Kakali, PhD thesis, NTU of Athens (1988).
15. V. Kasselouri and Ch. Ftikos, Cem. Concr. Research in press (1995).
16. E.F. Kaeble, Handbook of X-Rays, chapt. 17, p.4, McGraw-Hill (1967).
17. B.E. Waren, X-Ray Diffraction, Dover, p.251 (1990).